

# Temperature perturbations evolution as a possible mechanism of exothermal reaction kernels formation in shock tubes

A V Drakon, A D Kiverin and I S Yakovenko

Joint Institute for High Temperatures of the Russian Academy of Sciences, Izhorskaya 13  
Bldg 2, Moscow 125412, Russia

E-mail: alexeykiverin@gmail.com

**Abstract.** The basic question raised in the paper concerns the origins of exothermal reaction kernels and the mechanisms of detonation onset behind the reflected shock wave in shock-tube experiments. Using the conventional experimental technique, it is obtained that in the certain diapason of conditions behind the reflected shocks a so-called “mild ignition” arises which is characterized by the detonation formation from the kernel distant from the end-wall. The results of 2-D and 3-D simulations of the flow evolution behind the incident and reflected shocks allow formulation of the following scenario of ignition kernels formation. Initial stage during and after the diaphragm rupture is characterized by a set of non-steady gasdynamical processes. As a result, the flow behind the incident shock occurs to be saturated with temperature perturbations. Further evolution of these perturbations provides generating of the shear stresses in the flow accompanied with intensification of velocity and temperature perturbations. After reflection the shock wave interacts with the formed kernels of higher temperature and more pronounced kernels arise on the background of reactivity profile determined by moving reflected shock. Exothermal reaction starts inside such kernels and propagates into the ambient medium as a spontaneous ignition wave with minimum initial speed equal to the reflected shock wave speed.

## 1. Introduction

Nowadays the shock tube experiment is the most common technique for studying exothermal reactions. According to the ideal shock tube theory [1] the induction stage is volumetric and proceeds at constant temperature and pressure in the adiabatically compressed mixture behind the reflected shock. However, it is valid only for so called “strong ignition” regime. In case of low level of reactivity, e.g. at relatively low temperature behind the reflected shock, one can observe localized ignition inside kernels that is usually referred as “mild ignition” regime. For the first time such a regime of ignition was observed by Soloukhin in [2]. Such a regime is systematically observed in shock tubes with two-stage [2–5] and multi-stage compression [6], as well as in flow reactors [7] and rapid compression machines [8]. According to [9] the scenario with formation of ignition kernels and sequential mixture burning in flame regime fully determines the distinctions between kinetic calculations and experimental data at low temperatures. The calculations [9, 10] for different mixtures including  $\text{H}_2/\text{O}_2$ ,  $\text{H}_2/\text{CO}/\text{O}_2$  and  $\text{C}_3\text{H}_8/\text{O}_2$  are in a good agreement with this hypothesis. The origins of the ignition kernels is the key obstacle towards understanding of the “mild ignition” phenomenon, the overcoming of which should help



to get clear interpretation of the shock-tube experiments and to extract features of combustion kinetics out from the experimental data.

In [8] it was shown that the ignition of micro particles occasionally suspended in the reactive atmosphere has taken place prior to gas-phase ignition. The burning particles by themselves can cause the ignition kernels formation. But on the other hand they can merely visualize the position of ignition kernels whose origins are fully determined by the evolution of gasdynamical flows. Recent calculations [11,12] showed that ignition kernels in fuel–air mixtures can be formed in the vortical flows separated from the wall after reflected shock interaction with boundary layer. In case of argon-diluted mixtures the characteristic time of boundary layer diffusion is much greater and therefore there may be no vortices propagation inside the bulk flow on the time scales of shock-tube experiment. In this case the most heated region is the shear zone inside the boundary layer and this is where one should expect to observe ignition. Such a regime was obtained recently in experimental work [13]. However it should be noted that in [13] the emerging of ignition kernels was also connected with the presence of particles artificially suspended in the gaseous mixture by experimentalists. As these particles were able to provide local additional energy release due to friction or due to catalytic reactions on their surfaces the origin of the ignition kernels is not obvious. Actually, there is always some fraction of the particles inside the shock tube and therefore it is really hard to determine what factor plays a leading role, whether it is pure gasdynamics or gasdynamics of the flow with suspended particles. Besides the other physical mechanisms are possible such as impurity of the gaseous mixture [14], catalytic reactions on the walls etc.

It is also known that during and after the diaphragm rupture a set of non-steady gasdynamical processes are proceeding [15]. The transient jet flow generates oblique compression waves that are causing additional mixture heating in the regions of their reflections and interactions between each other. As a result the flow behind the incident shock occurs to be saturated with temperature perturbations localized on relatively small spatial scales. These temperature perturbations can be relatively strong on the early stage that can cause localized partial reactions and formation of active radicals. Afterwards the temperature perturbations attenuate and the radicals could not recombine until the temperature is raised again. Therefore the reflected shock propagates through the medium with non-uniform spatial distribution of temperature and active radicals. Further evolution of entropy perturbations in the flow behind the incident shock wave is the key physical mechanism. As these perturbations are having three-dimensional structure they act on the flow as a turbulizing grid generating the shear stresses in the flow driven by the directed flow. As a result, the process evolves in a regime close to Tollmien–Schlichting wave. Forming three-dimensional non-uniformities of the flow are characterized by the velocity and temperature perturbations rising in time. After reflection the shock wave interacts with these regions of higher temperature and more pronounced chemical kernels arise on the background of reactivity profile formed behind the moving reflected shock. It seems to be reasonable to analyze in details such a scenario as it can determine the possible mechanism of ignition kernels formation even in argon-diluted mixtures.

Analysis of the flow evolution behind the incident and reflected shocks on the basis of two- and three-dimensional computer simulations was carried out to get clear understanding of the ignition kernel origins. A set of experiments in stoichiometric hydrogen-oxygen argon diluted mixture aimed at extracting the range of parameters that corresponds to the “mild ignition” were performed and thoroughly analyzed. In the next section we represent the results of experimental analysis and formulate the possible scenario of ignition kernels formation as well as the problem setup for numerical simulations. Whereupon we discuss the numerical results in section 3 and conclude in section 4.

## 2. Problem setup

### 2.1. Experiments overview

Conventionally the pressure and OH emission or any other additional data are measured in the cross sections at some distance from the closed end-wall. Arrival of the incident and reflected shocks is registered by almost stepwise change in pressure value. The formed self-sustained detonation is also registered by the sharp pressure increase coupled with sharp increase in OH emission signal. Time period from shock reflection to the pressure spike recording is frequently identified as an induction delay time [16,17]. One can also observe that the coupled sharp increase in pressure and OH emission signal is usually preceded by slower increase in both signals on the background of almost constant values behind the reflected shock. The nature of such a primary pressure and emission rise is usually explained by pre-ignition energy release due to the partial reactions [17]. According to modern notions about induction phase of ignitions it is known that it proceeds at almost constant temperature or with negligible temperature increase never exceeding 5–10% of the ignition temperature. Therefore at the first sight such an explanation seems to be valid. However it contradicts the determination of the self-sustained detonation by which the induction phase starts behind the shock driving the detonation. Thus there should be another explanation of two phase rise of coupled pressure and OH emission signals that is consistent with the “mild ignition” concept of ignition birth inside localized kernels. It can be formulated as follows: the ignition starts inside the localized kernel and reaction wave propagates outwards from the ignition epicenter compressing the medium. As the ignition kernel is usually localized inside relatively small volume the reaction front does not spread over the whole cross-section of the shock tube therefore the registered signal of pressure and OH emission can be relatively low compare to the case of flame occupying the whole tube cross-section. The reaction front passes the registration section, accelerates and causes onset of a self-sustained detonation wave that returns to the registration section and causes the sharp increase of the signal. To register such a scenario one should consider a data from the set of spaced registration sections including the gauges directly on the end-wall surface.

Here we used a standard shock tube of total 4.5 m length with driver section of 1.5 m length. Shock tube diameter was 50.0 mm. Low pressure section was filled with test mixture at normal temperature and pressure  $\sim 100.0\text{--}400.0$  mbar. Driver section was filled with helium at about 4.8 bar pressure. Three pressure gauges were set on the end-wall and side wall at the distance of 13.0 and 107.0 mm out from the end-wall. OH emission was registered in the cross section at 13.0 mm distance from the end-wall. In 20% ( $2\text{H}_2 + \text{O}_2$ )/80% Ar mixture characteristic time scale of fine process observation was about 1200–1300 ms. It was found (figure 1) that regime with detonation formation at the distance from the end wall can be observed at the incident shock intensity corresponding to the ignition delay time of 600–800 ms. In figure 1a corresponding data is presented. The detonation wave first arrive to the most remote section (at 107 mm from the end-wall) and reaches the less remote section (at 13 mm) after about  $60\text{ }\mu\text{s}$ . Thus one can conclude that the formed detonation wave arises at some distance from the end-wall and then propagates towards it. Difference between time instances of detonation arrival to the section (13 mm) and to the end-wall allows to estimate the characteristic detonation speed which occurs to be about 1530.0 m/s and quite close to the available data for detonation velocities at obtained mixture state ( $T \approx 1052.0$  K,  $p \approx 6.67$  bar). Time-lag between two remote registration sections corresponds to the speed  $\approx 1570.0$  m/s. Hence one can conclude that the detonation onset takes place in the section nearby the most remote gauge and its position relative the end-wall can be estimated as  $\approx 105$  mm. However the position of the ignition epicenter is uncertain as the obtained data provide almost no information about the pre-detonation transient phases that can only be derived using either advanced experimental techniques or numerical simulations.

## 2.2. Setup and methodology for numerical simulations

In order to reproduce the ignition behind the reflected shock in conditions close to those described above the specific numerical problem setup was elaborated according to the scenario outlined in introductory section. We studied the flow of  $\text{H}_2/\text{O}_2/\text{Ar}$  gaseous mixture driven by the expanding He in the shock tube. Initial temperature was 300.0 K, pressure of reacting mixture was varied in the range of 0.3–0.4 bar and pressure of driver gas (He) was set at 3.5 bar. The initial conditions were set according to the approach proposed and used in [18]. Comparing images on figure 2 obtained numerically using this approach and experimental schlieren photos from [15] one can see qualitatively fair reproduction of the flow structure in the vicinity of the diaphragm section. Such a flow consists of expanding spherical shock close to that is formed immediately after the diaphragm rupture [15] and reproduced quite well when using either gradual model of diaphragm opening [19] or the model accepted here. While propagating inside the channel expanding waves generate temperature perturbations in the points of their interactions and reflection from the side walls. The maximal temperature in such a point achieves  $\sim 1000.0$  K. After a very short period (about several microseconds) this temperature relaxes to the ambient one transforming the excess entropy into the flow internal degrees of freedom. These entropy perturbations and their further evolution in the flow forming behind the shock wave determine the emergence of future ignition kernels. In this paper we solved two basic problems: (i) we analyzed the qualitative opportunities for temperature kernels formation in 3-D non-reactive calculations and (ii) we considered 2-D reactive full-scale calculations to analyze the peculiarities of ignition and detonation onset. To resolve the peculiarities of entropy perturbations evolution in the reacting flow one should solve full three-dimensional system of reactive Navier–Stokes equations for compressible viscous flow. The equations are as follows:

$$\frac{\partial \rho}{\partial t} + \text{div}(\rho \vec{u}) = 0, \quad (1)$$

$$\frac{\partial Y_i}{\partial t} + u_j \frac{\partial Y_i}{\partial x_j} = -\frac{1}{\rho} \frac{\partial}{\partial x_k} \left( \rho D_i \frac{\partial Y_i}{\partial x_k} \right) + \left( \frac{\partial Y_i}{\partial t} \right)_{\text{chem}}, \quad (2)$$

$$\frac{\partial u_i}{\partial t} + u_j \frac{\partial u_i}{\partial x_j} = -\frac{1}{\rho} \left[ \frac{\partial p}{\partial x_i} - \frac{\partial \sigma_{ij}}{\partial x_j} \right], \quad (3)$$

$$\frac{\partial E}{\partial t} + u_j \frac{\partial E}{\partial x_j} = -\frac{1}{\rho} \left[ \frac{\partial p u_i}{\partial x_i} - \frac{\partial \sigma_{ij} u_j}{\partial x_j} - \frac{\partial}{\partial x_i} \left( \kappa(T) \frac{\partial T}{\partial x_i} \right) - \rho \sum_k h_k \left( \frac{\partial Y_k}{\partial t} \right)_{\text{chem}} \right], \quad (4)$$

$$E = \epsilon + \frac{1}{2} \vec{u}^2, \quad (5)$$

$$\epsilon = c_V(T)T, \quad (6)$$

$$p = nRT, \quad (7)$$

$$\sigma_{ij} = \mu \left( \frac{\partial u_i}{\partial x_j} + \frac{\partial u_j}{\partial x_i} - \frac{2}{3} \delta_{ij} \frac{\partial u_k}{\partial x_k} \right), \quad (8)$$

where  $\rho$  is the mass density,  $p$  is the pressure,  $T$  is the temperature,  $\vec{u}$  is the mass velocity vector,  $Y_i$  is the mass fraction of  $i$ -th species,  $E$  and  $\epsilon$  are the specific full and internal energies,  $\sigma_{ij}$  is the viscous tensor,  $\mu$ ,  $\kappa$  and  $D_i$  are the transport coefficients of molecular viscosity, thermal conductivity and diffusivity of  $i$ -th species,  $n$  and  $c_V$  are the molar mass of the mixture and its specific heat at constant volume. Last term in equation (2) describes the chemical transformations in the reaction zone. To reproduce hydrogen combustion, reaction kinetics from [20] was used.

The equations were solved numerically using a numerical scheme of second order accuracy in space and first order accuracy in time. The usage of low-order numerical scheme excludes

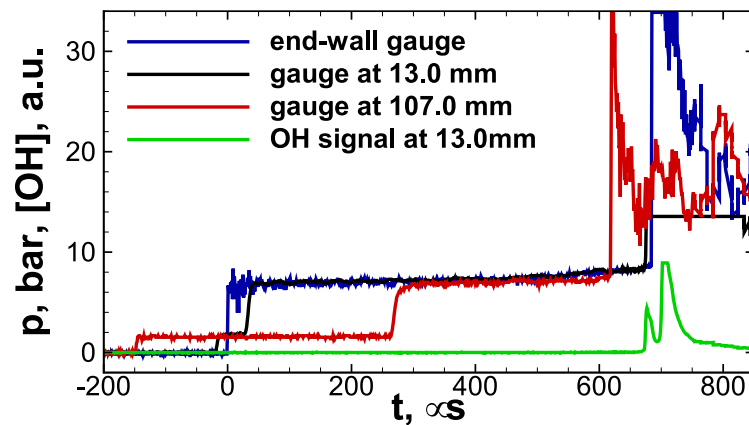


**Figure 1.** Pressure and OH emission profiles in different cross sections.

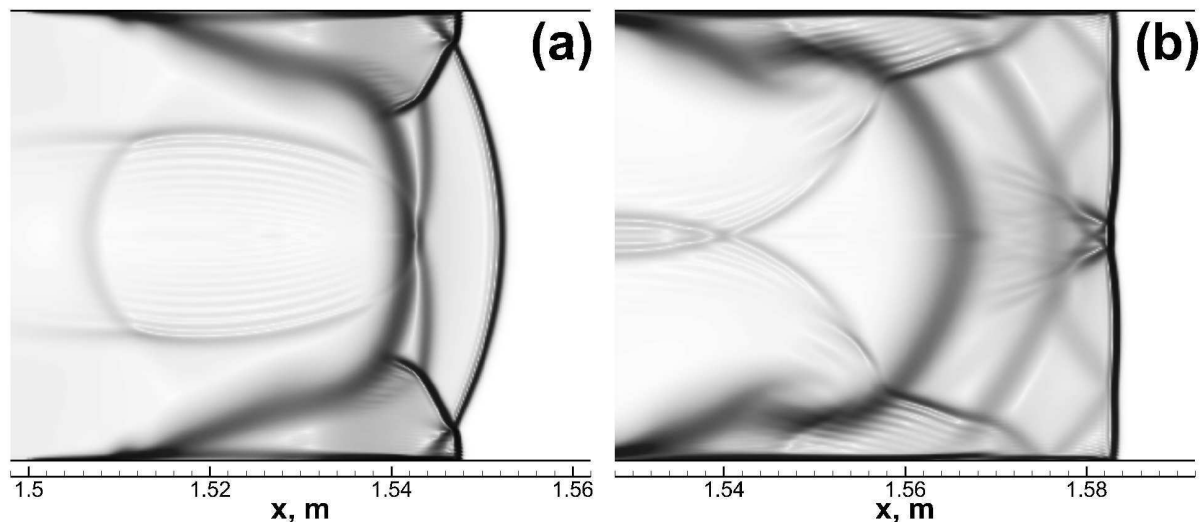


**Figure 2.** Calculated flow structure in the vicinity of the contact surface after 50.0 (a) and 100.0  $\mu\text{s}$  (b) after diaphragm rupture. The field of temperature (density) gradient is plotted to visualize the compression waves, shocks and contact surfaces.

the non-physical oscillations and does not require the utilization of specific limiters. However to diminish the role of scheme viscosity one should use fine enough computational grids to resolve important scales. In more details the justification of such an approach is presented in recent paper [21]. The basic aim of the current work was to analyze the evolution of the temperature perturbations in order to predict possible scenarios of ignition kernels formation. Considered resolution tests for un-reactive medium showed convergence for 0.1mm numerical cell size. For calculations with account of chemical reaction the resolution should be at least 5 times greater (0.02 mm). Due to this computational cost for 3-D modeling becomes too high and only 2-D case was solved using reactive model. Non-slip boundary conditions were applied for side walls to model the shear flows in the vicinity of the walls where the higher rate of temperature perturbations increase took place. In 3-D case the slip boundary conditions were applied and the self increase of the perturbations was analyzed for qualitative understanding of the opportunities.

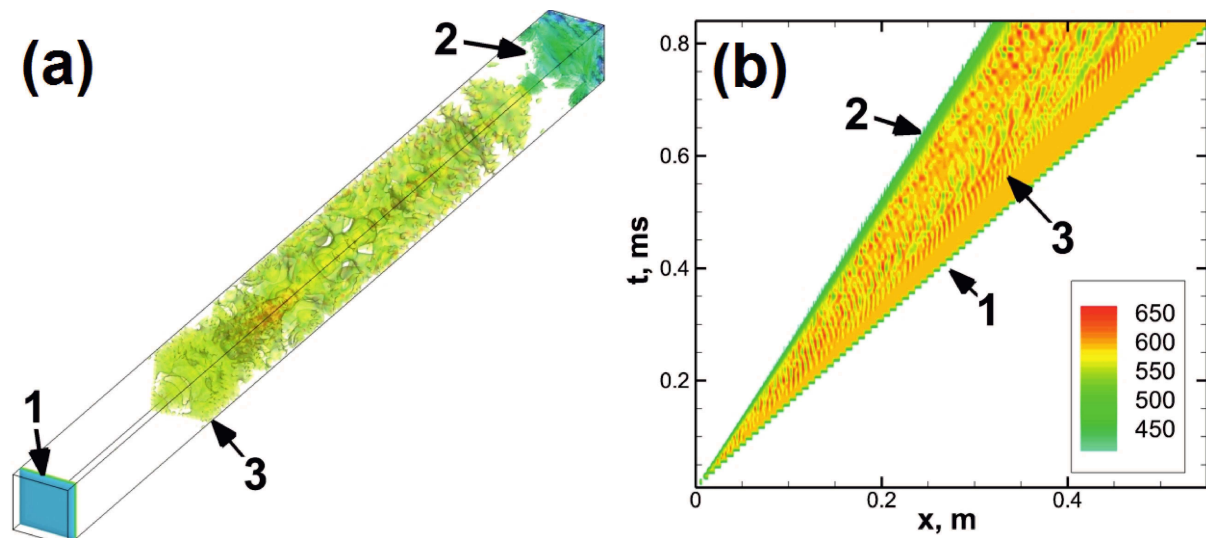


**Figure 3.** (a) Characteristic flow pattern between the shock wave and contact surface. The iso-surfaces of specific Q-criterion show the vortical structures forming as a result of shear flow evolution. Color represents the temperature field (similar as on the right frame). (b)  $x$ - $t$  diagram of the flow between the shock wave and contact surface. 1—incident shock wave, 2—contact surface, 3—perturbations wave front.

### 3. Results and discussion

#### 3.1. Conceptual 3-D scenario of kernels formation due to the temperature perturbations evolution

Consider the flow pattern between the incident shock wave and contact surface. According to the scenario formulated above the temperature perturbations formed due to the non-steady evolution of test mixture flow during and after the diaphragm rupture cause generation of shear flows. According to the carried 3-D calculations it was obtained that further evolution of these shear flows causes birth of vortical structures mixing the compressed mixture (see figure 3a). Due to the mixing and flow kinetic energy dissipation into the heat the hot regions are formed on the background of almost constantly heated compressed mixture. The flow of compressed gas is accelerating and the lag between the shock front and the perturbed medium reduces down to asymptotically constant finite value. The estimate of temperature perturbations magnitude does not exceeds  $\sim 50.0$  K which, however, almost doubles after the interaction with the reflected flow and can become the origin of the ignition kernel. In 2-D case the rate of temperature perturbations rise occurs to be much less (about an order of magnitude) than in 3-D case however there is always a natural shear flow inside a boundary layer which was simulated using no-slip boundary conditions for 2-D reactive calculations presented in the next section.

#### 3.2. Ignition kernels formation in 2-D reactive model

Let us now consider in details the evolution of the ignition kernels on the basis of 2-D calculations of the full-scale problem. As it was already confirmed above there are feasible opportunities for temperature perturbations birth and rise in the flow behind the shock wave. According to this the rates of pre-ignition (mostly endothermic) reactions should be larger inside these local hot spots. After shock wave reflection from the end-wall the reaction starts in the Lagrangian particle situated directly on the end-wall. The temperature and pressure are higher behind the reflected shock so the rates of endothermic reactions on the end-wall should be greater than in remote Lagrangian particles. However one should take into account higher reaction rate in the

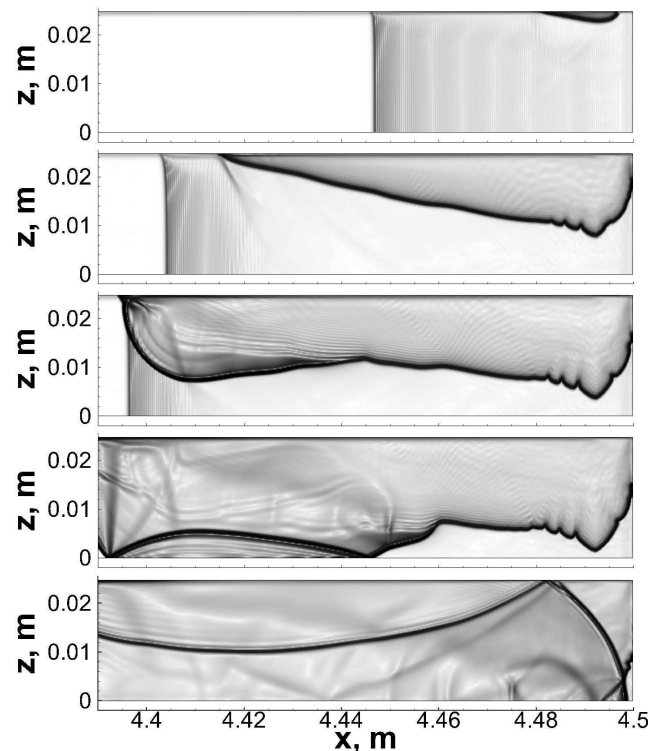


**Figure 4.** Density gradient field illustrating the flow evolution in the vicinity of ignition kernel.  $U_{IS} = 683.0$  m/s. Sequential time instants after ignition start are:  $30 \mu s$ ,  $140 \mu s$ ,  $160 \mu s$ ,  $170 \mu s$ ,  $200 \mu s$ .

Lagrangian particles moving together with the hot spots after their interaction with the reflected shock wave. Considering higher reaction rate and previous reaction history the scenario can be proposed according to which the Lagrangian particle moving together with the hot spot can be ignited earlier than that situated directly on the end-wall. As the only possibility of hot spot formation in the considered 2-D case is due to additional heating inside the boundary layer and there is almost no vortices breakaway into the bulk flow (due to the argon dilution) the most probable ignition kernel position is inside the narrow boundary layer near the side wall. The evolution of the ignition kernels for two cases with different incident shock velocities of  $U_{IS} = 683.0$  m/s and  $U_{IS} = 671.0$  m/s are presented correspondingly in figures 4 and 5. Corresponding pressure profiles on three gauges are presented in figures 6 and 7.

In case represented in figures 4 and 6 the background temperature behind the reflected shock is about 920.0 K and the exothermal reaction starts first in the hot region at  $\sim 14.0$  mm from the end-wall at  $\sim 20 \mu s$  after the shock reflection. The reaction wave propagates after the reflected shock with acceleration (that will be additionally discussed in the next subsection) and forms a detonation wave at  $\sim 96.0$  mm directly behind the outrunning shock at  $\sim 140 \mu s$  after ignition. In other directions no reaction wave acceleration is observed, therefore the regions of un-reacted medium remains between the end-wall and position of detonation onset. Thereby the detonation front can propagate towards the end-wall. At first the detonation wave is registered on the most remote gauge at 104.0 mm distance from the end-wall, and after it is registered on the less remote gauge and finally on the wall. Qualitatively this regime of ignition is similar to that observed experimentally (see figure 1). Quantitative differences relate to the overestimated additional heating inside the shear boundary layer due to artificially high viscosity provided by numerical discretization and rude no-slip boundary condition.

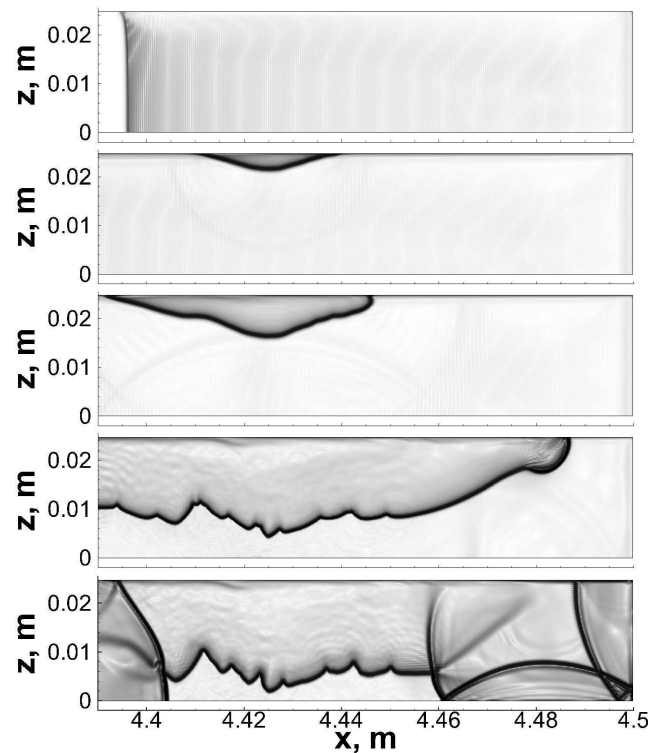


**Figure 5.** Density gradient field illustrating the flow evolution in the vicinity of ignition kernel.  $U_{IS} = 671.0$  m/s. Sequential time instants referent to the ignition start are:  $-70 \mu s$ ,  $30 \mu s$ ,  $80 \mu s$ ,  $200 \mu s$ ,  $220 \mu s$ .

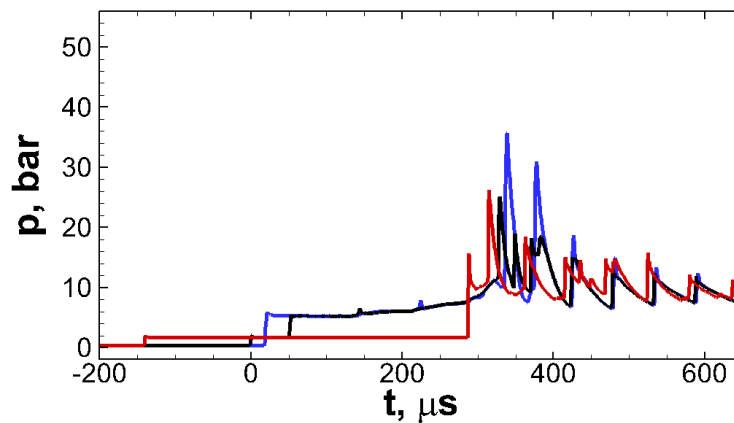


**Figure 6.** Pressure gauges signals.  $U_{IS} = 683.0$  m/s.

In the second case represented in figures 5 and 7 the background temperature behind the reflected shock is about 905.0 K and the position of ignition kernel is  $\sim 75.0$  mm distant from the end-wall. Position of the detonation onset is  $\sim 168.0$  mm distant from the end-wall. Besides there is one more source of detonation emerging on the reaction front that propagates from the ignition kernel towards the end-wall. Compression waves irradiated by the reaction front and then reflected from the end-wall and side walls of the tube cause counter flows that strongly influence the conditions of reaction front evolution here. Second detonation origin is at  $\sim 15.0$  mm far from the end-wall. Therefore there are discrepancies in readings by the gauge



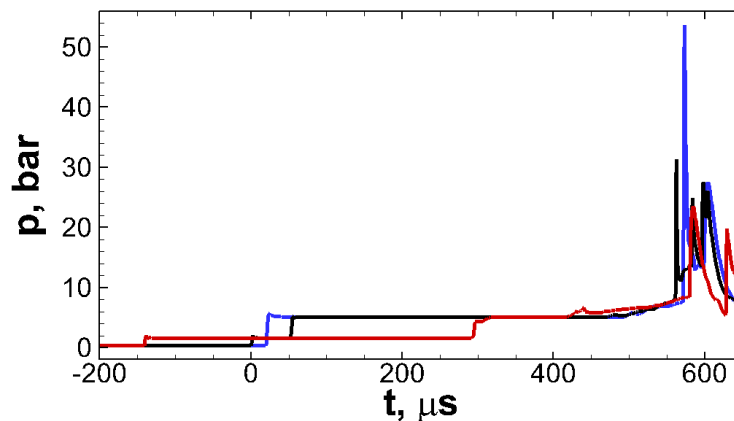


**Figure 7.** Pressure gauges signals.  $U_{IS} = 671.0$  m/s.

at 13.0 mm from the end-wall and the most remote gauge at 107.0 mm from the end-wall that register two independent detonation waves.

At lower temperatures behind the reflected shock wave (less than 890.0 K) no ignition and correspondingly no detonation onset were observed on the characteristic scales of the shock tube experiment. At temperatures higher than  $\sim 1100.0$  K a regime of “strong ignition” directly behind the reflected shock was observed.

### 3.3. Ignition kernels evolution and detonation onset

Consider separately the mechanism of detonation formation. As it was mentioned above the ignition starts inside the region with local temperature value higher than in the environmental medium compressed behind the reflected shock. The formed reaction wave propagates outwardly from the ignition zone through the compressed and correspondingly heated mixture that determines a relatively high burning velocity which according to [22] can be defined as intermediate asymptotic solution of the steady flame propagation problem. In presence of non-uniform profile of reactivity such a reaction wave can be defined as a so-called “spontaneous combustion wave” which dynamics is fully determined by the character of the non-uniformity [23]. In cases represented in figures 4 and 5 a non-uniformity of reaction progress variable is determined by the consequential compression by the incident and reflected shocks. In case of fully frozen kinetics behind the incident shock a minimal reaction wave velocity in the direction after the reflected shock can be estimated as a reflected shock speed. In more realistic case the reaction progress is increasing in the direction of contact surface and therefore the velocity should be greater and should increase as the reaction wave propagates after the reflected shock. Besides in case of sub-sonic initial velocity of the reaction wave the compression waves irradiated by the propagating reaction zone and then reflected from the side walls and end-wall are effecting the reaction wave propagation causing additional acceleration. After achieving the local sonic speed the reaction wave together with the compression waves irradiated from the reaction zone are able to produce detonation similar to the scenario first proposed in [24] for case of deflagration-to-detonation transition in a consequence of flame acceleration in channel. The illustration of this event occurring after the reaction wave acceleration is given in figure 8 where temperature and pressure profiles in the section along the side walls are presented at different time instants. Figure 9 represents a reaction wave velocity evolution for two cases of “strong” and “mild” ignition. The latter one corresponds to the case presented in figures 4 and 6. One can observe that in case of “mild ignition” all the factors described above determine a non-steady behavior of the reaction wave propagation regime. However the average pattern of velocity rise is almost

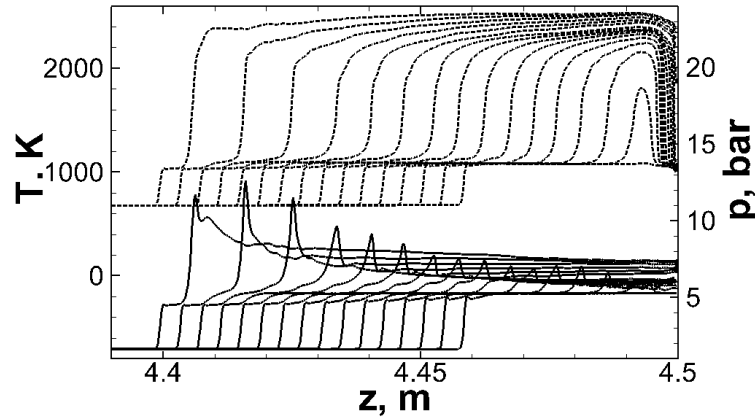


**Figure 8.** Reaction wave evolution and detonation onset. Temperature (dashed) and pressure (solid) profiles are presented at sequential time instants equally spaced ( $\Delta t = 10 \mu s$ ) after the ignition start inside the hot spot.  $U_{IS} = 683.0$  m/s.

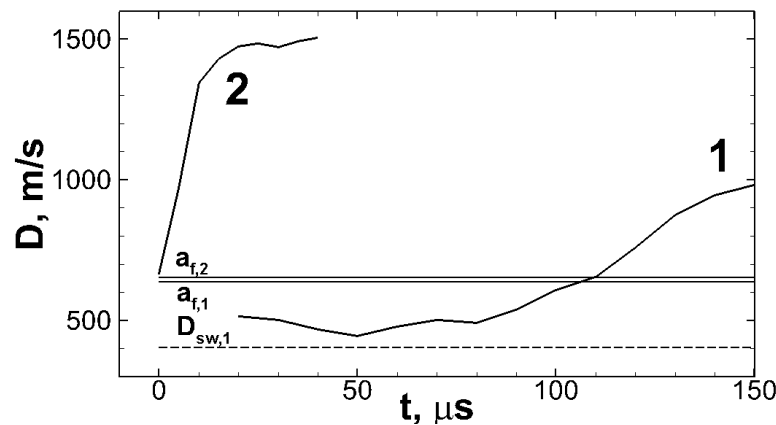


**Figure 9.** Reaction waves velocities evolutions for two regimes of “mild” 1 ( $U_{IS} = 683.0$  m/s) and “strong” 2 ( $U_{IS} = 760.0$  m/s) ignition.  $a_{f,1}$  and  $a_{f,2}$  are sonic speeds in the compressed mixture behind the reflected shock for two cases correspondingly.  $U_{RS,1}$  is a reflected shock velocity in case 1.

exponential that illustrates the presence of a positive feedback between the propagating reaction front and all of the factors peculiar to the propagation regime. According to this let us write an acceleration law as:

$$D = D_0 \exp \left( \frac{D_0 t}{\alpha H} \right), \quad (9)$$

where  $D$  is a reaction wave velocity,  $D_0$  is initial reaction wave velocity and  $\alpha H$  is a characteristic spatial scale of the order of tube diameter  $H$ . According to this law one can obtain an expression for pre-detonation distance which is estimated as a distance from the ignition epicenter to the point where the reaction wave velocity achieves the sonic speed in the combustion products  $a_b$  [25]:

$$L_D \approx \alpha H \frac{a_b}{D_0}. \quad (10)$$

Calculated values for  $\alpha$  for cases considered here are presented in figure 10. One can see that  $\alpha$  is of the order of unity in the range where “mild ignition” and sequential onset of

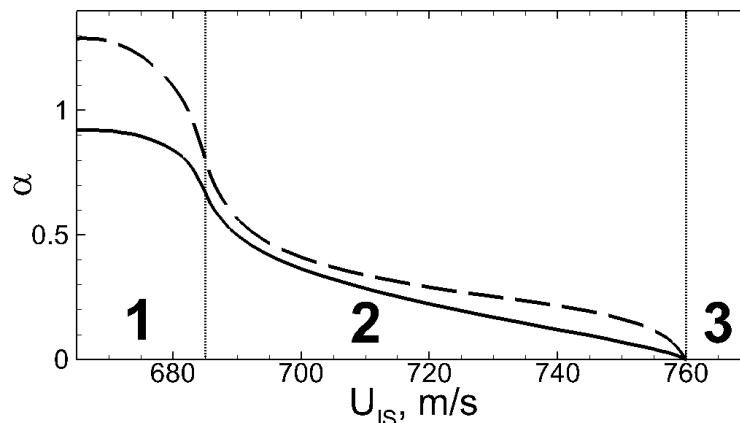


**Figure 10.** Reaction wave acceleration rate  $\alpha$  versus incident shock velocity. Labels 1, 2 and 3 show the regions corresponding to three regimes of detonation onset: 1—due to reaction wave acceleration; 2—due to shock-to-reaction wave interaction; 3—due to “strong ignition” behind the reflected shock.

detonation takes place according to the scenario described above (region 1).  $\alpha$  drops down with the increase of incident shock intensity in region 2 where the detonation onset takes place as a result of interaction between accelerating reaction wave and the reflected shock. In the region 3 a “strong ignition” regime was observed characterized by the immediate detonation onset directly behind the reflected shock (see curve 2 in figure 9) and no reaction wave acceleration stage. Solid and dashed lines in figure 10 represent the estimation (10) in which  $D_0$  equals  $D(t = 0)$  and  $U_{RS}$  (reflected shock speed) correspondingly. One can see that difference between two estimations reduces in the region 2 that is due to the switch of the detonation onset mechanism from reaction wave acceleration to the shock-to-reaction wave interaction. The sufficient reduction in the time-spatial scales of detonation onset here can result in the interpretation of such regimes as “strong ignition”.

#### 4. Conclusions

The obtained results allow to formulate a possible scenario of “mild ignition” evolution including the origins of ignition kernels and the mechanisms responsible for detonation formation far from the end-wall of the shock tube. Analysis of three-dimensional pattern of the flow evolving behind the incident shock showed possible opportunities of hot spot formation due to the temperature perturbations evolution in the shear (vortical) flows. Herewith both temperature perturbations and shear flows are the sequences of non-steady flowing of the driver gas into the test mixture through the rupturing diaphragm. The formed hot spots are intensified by the reflected shock and are able to give birth to the local ignition at some distance from the end-wall. The minimal value of reaction wave velocity can be estimated as a reflected shock wave speed however in most cases it is higher, but bounded above by the local sonic speed value. Thus the onset of detonation becomes possible only as a sequence of reaction front acceleration that however is quite intrinsic to the conditions formed in the gap between the end-wall and outrunning reflected shock wave. The position of ignition kernel formation can be estimated using the registration data from several pressure transducers and assumption of almost exponential law of reaction wave acceleration. Knowing the position of ignition kernel a true ignition delay time can be measured. It should be noted however that it will be always shorter than that estimated for the classical value of temperature behind the reflected shock as it corresponds to more violent conditions realized inside the formed hot spot. To achieve higher accuracy of the experimental

data one should more thoroughly analyze the peculiarities of hot spots formation. On the basis of numerical results and recent experiments [13] it can be also concluded that for case of argon-diluted mixtures the possibilities of ignition kernel formation are closely connected with boundary effects on the side surfaces of the tube and/or on the surfaces of suspended solid particles.

The proposed physical mechanisms are general and can be used to interpret the experimental data in other systems with delayed exothermal reaction start including the pure mixtures (with no inert gas dilution), the systems with multi-stage compression and even the systems filled with oxygen-free mixtures in which the exothermal effects take place not due to the combustion reaction but due e.g. the formation and growth of the soot particles. The latter case can be confirmed by the plotting the wave velocities evolutions for “strong” and “mild” regimes of condensation wave formation presented in [26] which will provide almost the same pattern as presented in figure 9.

### Acknowledgments

The work was funded by grant MK-8693.2016.2 for the state support of young Russian scientists. We acknowledge support of the Joint Super Computer Center of Russian Academy of Sciences. We also appreciate fruitful discussions with our colleagues and especially grateful to professor A V Eremin and professor M F Ivanov.

### References

- [1] Zel'dovich Ya B and Raiser Yu P 1966 *Physics of Shock Waves and High-Temperature Hydrodynamic Phenomena* (New York: Academic Press)
- [2] Zaytzev S G and Soloukhin R I 1961 *Proc. Symp. (Int.) Combustion* **8** 344
- [3] Petersen E L *et al* 2007 *Combust. Flame* **149** 244
- [4] Blumenthal R, Fieweger K, Komp K H and Adomeit G 1996 *Combust. Sci. Technol.* **113** 137–166
- [5] Gelfand B E *et al* 2000 *Shock Waves* **10** 197
- [6] Medvedev S P 2012 *15th International Symposium on Flow Visualization* (Minsk, Belarus: ITMO NASB)
- [7] Schonborn A *et al* 2014 *Int. J. Hydrogen Energy* **39** 12166
- [8] Shushkov S V *et al* 2012 *J. Eng. Phys. Thermophys.* **85** 867
- [9] Medvedev S P *et al* 2010 *Combust. Flame* **157** 1436
- [10] Agafonov G L and Tereza A M 2015 *Russ. J. Phys. Chem. B* **9** 92
- [11] Grogan K P and Ihme M 2015 *Proc. Comb. Inst.* **35** 2181
- [12] Khokhlov A, Austin J and Knisely A 2015 *25th ICDERS, August 2–7, 2015 Leeds, UK* 0020
- [13] Hanson R K and Davidson D F 2015 *25th ICDERS, August 2–7, 2015 Leeds, UK* 0260
- [14] Gelfand B E *et al* 1996 *Dokl. Akad. Nauk* **349** 482
- [15] Pakdaman S A 2014 Ph.D. thesis Univ. Calgary
- [16] Burke S M *et al* 2015 *Combust. Flame* **162** 296
- [17] Pang G A, Davidson D F and Hanson R K 2009 *Proc. Comb. Inst.* **32** 181
- [18] Tertashima H *et al* 2014 *Int. J. Hydrogen Energy* **39** 6013
- [19] Petrie-Repar P J 1997 Ph.D. thesis Mechanical Engineering, University of Queensland
- [20] Kusharin A Y *et al* 1998 *Comb. Sci. Tech.* **34** 85
- [21] Ivanov M F, Kiverin A D and Liberman M A 2015 *Combust. Flame* **162** 3612
- [22] Zel'dovich Ya B 1980 *Combust. Flame* **39** 219
- [23] Zel'dovich Ya B 1980 *Combust. Flame* **39** 211
- [24] Ivanov M F *et al* 2010 *Dokl. Akad. Nauk* **434** 756
- [25] Ivanov M F, Kiverin A D and Yakovenko I S 2015 *J. Phys.: Conf. Ser.* **653** 012062
- [26] Emelianov A V, Eremin A V and Fortov V E 2010 *Pis'ma Zh. Eksp. Teor. Fiz.* **92** 101